ELSEVIER

Polymer 40 (1999) 6321–6327

polymer

Effect of a functional triblock elastomer on morphology in polyamide 6/polycarbonate blend

Chang Hyung Lee[a], Yong Moo Lee[b], Hyeong Ki Choi[b,*], Shin Horiuchi[c], Takeshi Kitano[c]

[a]*Medical Devices and Radiation Health Department, Korea Food and Drug Administration, 5 Nokbeon-dong, Eunpyung-ku, Seoul, South Korea*
[b]*Department of Chemistry, National Institute of Technology and Quality, 2 Jungang-dong, Kwacheon City, Kyunggi-do 427 010, South Korea*
[c]*National Institute of Materials and Chemical Research, 1-1 Higashi, Tsukuba, Ibaraki, Japan*

Received 17 August 1998; received in revised form 26 October 1998; accepted 24 November 1998

Abstract

Morphology on the 75/25 polyamide 6 (PA6)/polycarbonate (PC) blends with various ratios of maleic anhydride functionalized poly-[styrene-b-(ethylene-co-butylene)-b-styrene] (SEBS-gMA) to poly[styrene-b-(ethylene-co-butylene)-b-styrene] (SEBS) was investigated by transmission electron microscopy, differential scanning calorimetry and small angle X-ray scattering. The total amount of added SEBS-gMA and SEBS was held constant at 20 parts hundred resin, (phr) i.e. 20 g against 100 g of the total amount of PA6 and PC). The 75/25 PA/PC blend with 0/20 SEBS-gMA/SEBS showed a co-continuous phase structure. The co-continuous phase morphology is one of the hallmarks of spinodal decomposition (SD), which takes place in the partially miscible system. It has been known that a binary blend of PA6/PC is completely immiscible at all temperatures. In contrast, the 75/25 PA/PC blends with 5/15, 10/10 and 20/0 SEBS-gMA/SEBS showed dispersed PC macrodomains and SEBS/SEBS-gMA microdomains in the PA6 matrix, indicating that these blends are totally immiscible. On blending with 0/20 SEBS-gMA/SEBS, the PA6 crystallinity and crystallization temperature (T_c) were lower than in other blends and the periodic regularity of SEBS-gMA/SEBS microphase separation was higher. In the other blends, the crystallinity and T_c was high and the periodic regularity of SEBS-gMA/SEBS microphase separation was low. This behavior is believed to arise from the different phase morphology formed on changing the ratio of SEBS-gMA to SEBS.

Keywords: Polyamide 6; Polycarbonate; Morphology

1. Introduction

Polyamide 6 (PA6) is well known for its excellent mechanical properties and good solvent resistance and is used in engineering applications. It is especially suitable as matrix material for thermoplastic compositions because of its good adhesion to glass and carbon fiber. PA6 is semi-crystalline thermoplastic polymer with a T_g of 50°C and a melting point of the main crystallites around 270°C depending on the thermal history [1]. Polycarbonate (PC) is an amorphous polymer with a high T_g of 148°C [1]. It is insensitive to moisture and durable to various weathering conditions. Taking this into account, it is very logical to consider whether they may complement each other in a blend, overcoming the drawbacks, while maintaining good properties. Therefore, blending of PA6/PC has been widely studied in various industrial fields.

PA6/PC blends are incompatible and immiscible in the whole range of composition and temperature [1,2]. Immiscible blends often have poor mechanical properties because of poor adhesion at the interface. For the improvement of interfacial conditions in PA6/PC blends, Horiuchi et al. [3–5] reported that certain combination of maleic anhydride functionalized poly[styrene-b-(ethylene-co-butylene)-b-styrene] (SEBS-gMA) and poly[styrene-b-(ethylene-co-butylene)-b-styrene] (SEBS) can be used effectively. They concluded that the dramatic improvement of impact strength can be achieved in 75/25 PA6/PC blends when the total amount of added SEBS-gMA and SEBS are held constant at 20 parts hundred resin (phr) and the ratios of SEBS-gMA to SEBS are varied [4]. These results were attributed to the encapsulation by SEBS-gMA or SEBS around PC domains in the PA6 matrix. However, the crystalline structure of PA6 matrix in PA6/PC blends may also affect material properties. It is widely accepted that properties of the blend in crystalline polymer/non-crystalline polymer blend depend on their crystalline structure. Coppola et al. [6] found a very close correlation between crystallization condition and mechanical property in a polypropylene (PP)/ethylene–propylene-rubber (EPR) blend. The formation of the

* Corresponding author.

0032-3861/99/$ - see front matter
PII: S0032-3861(98)00854-4

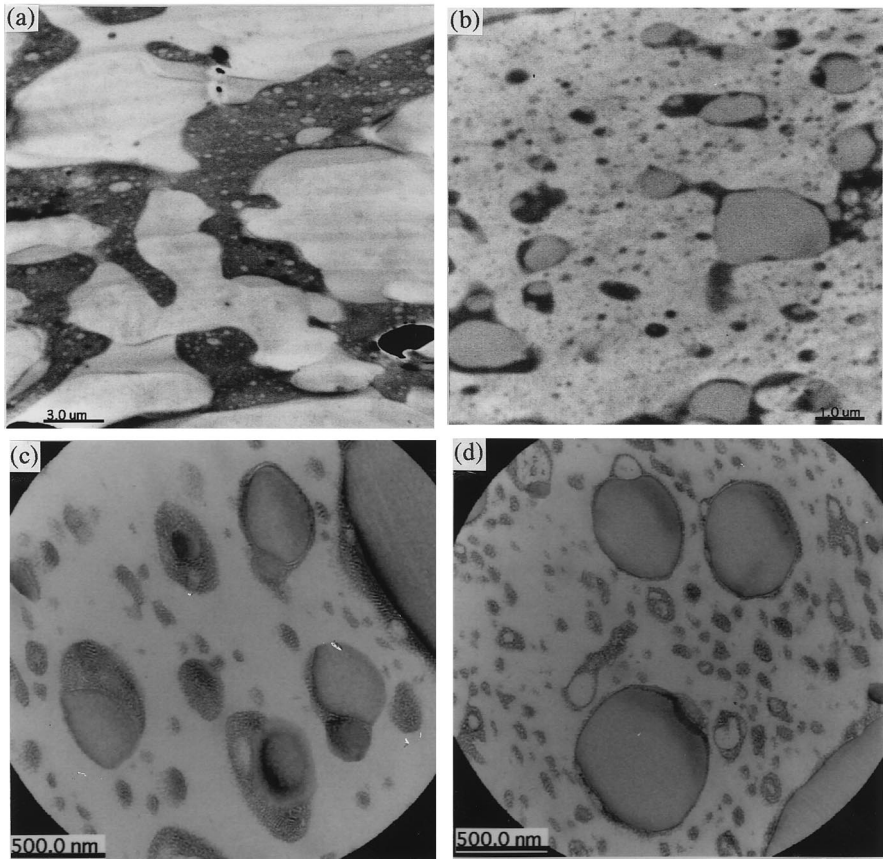

Fig. 1. TEM micrographs in 75/25 PA6/PC blends: (a) 0/20; (b) 5/15; (c) 10/10 and (d) 20/0 SEBS-gMA/SEBS. (c) and (d) are reproduced from Ref. [4].

crystalline structure relates to phase morphology. Therefore, we need to have information on both phase and crystalline morphology which will result in control of physical properties of the materials. This is motivated to investigate the crystalline and phase structure in 75/25 PA6/PC blends with the addition of SEBS-gMA/SEBS.

2. Experimental

2.1. Materials

All materials used in this work are supplied from commercial sources. PA6 is a hydrolytic poly (ϵ-caprolactam) (A1030BRF, Unichika Co.) with a number average molecular weight of 22 500 and a melting flow rate of 4.3. The concentration of the amine end group was determined as 5.0×10^{-5} mol g^{-1} by titration. Bisphenol-A PC was supplied by Teijin Chemical Co. Ltd., product name Panlite L-1250Y. These two polymers were dried at 80°C for at least 12 h in a vacuum oven to remove absorbed water before processing. The triblock copolymer, SEBS, is incorporated into the blends of PA6 and PC for compatibilizing of this system. This copolymer has styrene end blocks and a hydrogenated butadiene midblock resembling an ethylene/butylene copolymer. The SEBS functionalized with 2 wt.% MA onto the hydrocarbon chains, designated SEBS-gMA, is Kraton 1901, supplied by Shell, with a molecular weight of 20 000 and a styrene content of 29 wt.%. Unmodified SEBS is Kraton 1652 with the same molecular weight and styrene contents as Kraton 1901.

The dramatic improvement of impact strength can be achieved in 75/25 PA6/PC blends when the total amount of added SEBS-gMA and SEBS is held constant at 20 phr and the ratio of SEBS-gMA to SEBS is varied [4]. Hence, in this article, we will confine our discussion to 75/25 PA6/PC blends with the various ratios of SEBS-gMA to SEBS. The total amount of added SEBS-gMA and SEBS is held constant at 20 phr.

2.2. Blending procedures

The blend was prepared by extruding the components with a twin-screw extruder at about 290°C, using Plasticorder PL2000. After extrusion, the blend was cooled to room temperature and granulated to pellets. The blend sample was then injected into a mold using Autoshot-model 100B. The molded specimen was used for small angle X-ray scattering (SAXS), differential scanning calorimetry (DSC) and transmission electron microscopy (TEM).

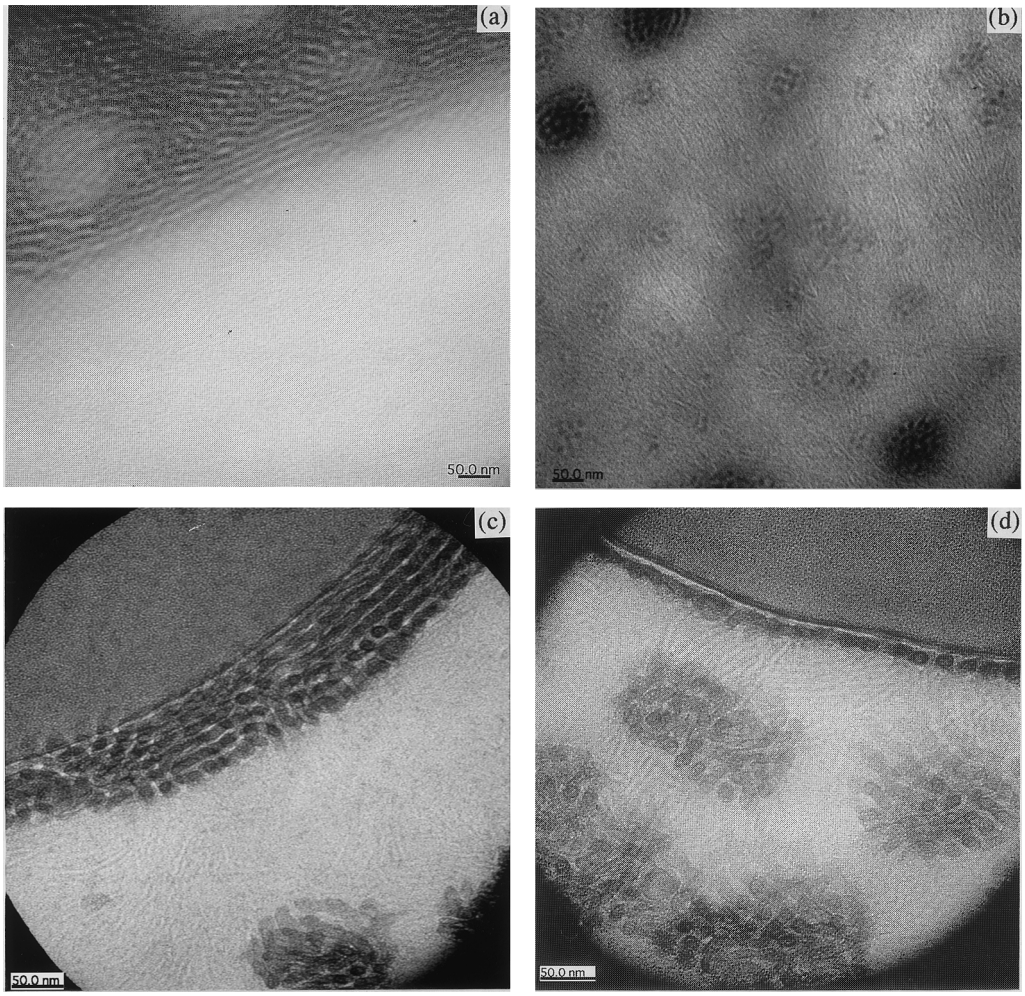

Fig. 2. Higher magnification view of TEM micrographs in 75/25 PA6/PC blends: (a) 0/20; (b) 5/15; (c) 10/10 and (d) 20/0 SEBS-gMA/SEBS. (c) is reproduced from Ref. [4].

2.3. Small angle X-ray scattering measurements

The X-ray beam was from synchrotron radiation; beam line 3C2 at Pohang Accelerator Laboratory, Pohang, South Korea. The storage ring was operated at an energy level of 2 GeV. The SAXS employs a point focusing optics with a Si double crystal monochromator followed by a bent cylindrical mirror. The incident beam intensity of 0.149 nm wavelength was monitored by an ionization chamber for the correction of minor decreases of the primary beam intensity during the measurement. The scattering intensity was detected with a one-dimensional position sensitive proportional counter with 1012 channels.

The scattering intensity, I, was corrected for background scattering. The scattering intensity by thermal fluctuations was then subtracted from the SAXS profile $I(q)$ by evaluating the slope of a $I(q)q^4$ versus q^4 plots [7] at wide scattering vectors q, where q is $(4\pi/\lambda)\sin\theta$, λ and 2θ being the wavelength and scattering angle, respectively. The correction for smearing effect by the finite cross section of the incident beam was not necessary for the optics of SAXS with point focusing.

2.4. Differential scanning calorimetry measurements

The thermal behavior of the blends taken from the injection molded specimen was examined by DSC. A DuPont DSC 10 equipped with a Thermal Analyst 2000 was used to obtain the DSC thermograms at a heating rate of 10°C min^{-1} and was calibrated with indium. The scans were run with samples ranging from 10 to 15 mg from 30°C to 300°C under a nitrogen purge to prevent oxidative degradation. All samples were heated to above melting, held at 300°C for 2 min to render the samples completely melted, and cooled from the melt with a cooling rate of 2°C min^{-1}.

2.5. Transmission electron microscopy measurements

TEM observation was carried out using a Zeiss CEM 902 at an accelerating voltage of 80 kV with an attached integrated electron energy loss spectrometer to perform the energy-filtering TEM. Sections were microtomed from

Table 1
The lamellar thickness *d*, the long period *L*, and the linear crystallinity *w* (Eq. (1)) in 75/25 PA6/PC blends by changing the ratio of SEBS-gMA/SEBS

SEBS-gMA/SEBS	*d* (nm)	*L* (nm)	*w*
20/0	4.9	9.1	0.54
5/15	5.0	7.9	0.63
10/10	4.9	8.0	0.61
0/20	4.8	7.4	0.65

molded samples perpendicular to the flow direction, and then stained with ruthenium tetraoxide (R_uO_4). Staining agents were used as aqueous solution of 0.5 wt.% R_uO_4.

3. Results and discussion

3.1. Morphology investigation

3.1.1. Transmission electron microscopy

Fig. 1 shows the TEM photographs of 75/25 PA6/PC blends with 0/20, 5/15, 10/10 and 20/0 SEBS-gMA/SEBS, where R_uO_4 is used for staining which is selective for the amorphous material. In 75/25 PA6/PC blends with 5/15, 10/10 and 20/0 SEBS-gMA/SEBS, the big PC macrodomains and small SEBS/SEBS-gMA microdomains are dispersed in the PA6 matrix (Fig. 1(b)–(d)). This indicates that these blends are totally immiscible. Blending of completely immiscible polymers exhibits two or more isolated domains in a matrix.

The phase morphology in 75/25 PA6/PC blend with 0/20 SEBS-gMA/SEBS is quite different from that of the other blends, as shown in Fig. 1(a). The PC-rich phases with SEBS/SEBS-gMA and PA6-rich phases are observed as dark and white zones, respectively, because the samples were stained by R_uO_4. Note that crystal lamellae appeared in white zones (see higher magnification views in Fig. 2(a)). One sees a high level of connectivity of both phases (dark and white zones) and their regular spacing of the phases. The two-phase structure with a unique periodicity and phase connectivity is one of the hallmarks of SD, i.e., macrophase separation, which takes places in the partially miscible system, i.e. lower critical solution temperature (LCST)/upper critical solution temperature (UCST). One possible explanation could be that LCST might be elevated over the barrel temperature under the high shear rate in extruder, and therefore, blending could be done in one phase region. Inoue et al. [8–10] reported that a connective structure in PC/poly (butylene terephthalate) (PBT) and PC/poly(styrene-*co*-acrylonitrile) (SAN) blend, is formed by shear-induced miscibility. Therefore one can speculate that this blend composition is miscible when mixed at high shear rate, and SD occurs in the static state. It is presently unclear why phase diagrams are so sensitive to the ratio of SEBS-gMA/SEBS. A scenario of the melt extrusion to yield the connective structure may be given as follows.

Under the high shear rate in the extruder, phase diagram elevated over the barrel temperature and one phase region becomes wide. Thus, the blend could be done in a wide temperature window for dissolution to get a homogeneous mixture. However, once the melt is extruded out from the nozzle, the shear rate turns out to be zero and LCST will immediately go down to the state without shear so that the SD will proceed until the system is cooled down to PA crystallization. The crystallization prevents further SD phase separation. Finally the melt injected sample shows a high level of connectivity of both phases.

The higher magnification view of TEM photographs is shown in Fig. 2. In 75/25 PA6/PC blends with 5/15, 10/10 and 0/20 SEBS-gMA/SEBS blends, SEBS/SEBS-gMA forms the macrodomains with diameters on the order of submicron dimensions on PA6 matrix (Fig. 2(b)–(d)). The microdomains are microphase-separated and the periodic length of the microphase separation are almost constant at around 24 nm on changing the ratio of SEBS-gMA to SEBS. The regularity of the microdomain is low. This may be ascribed to the PA6 crystallization, as the microdomains of SEBS-gMA/SEBS exist on the PA matrix so that the PA6 crystallization during cooling after extrusion may disorder the regularity of the microphase-separated structure.

However, in 75/25 PA6/PC blend with 0/20 SEBS-gMA/SEBS, SEBS-gMA/SEBS does not exhibit the dispersed microdomain structure on PA6-rich phases, but consists of one phase together with PC component (dark region in Fig. 2(a). The regularity of the microphase separation is higher than that in the other blends. The regularity should be less dependent on the PA6 crystallization, as SEBS-gMA/SEBS exists on PC-rich phases. This point will be discussed in more detail in Section 3.1.2.

As the staining medium penetrates only into the amorphous regions in the PA matrix, the PA crystalline lamellae appear as white stripes in Fig. 2. The lamellar thickness *d* and long period between crystalline lamellae *L* is calculated from TEM. The results are summarized in Table 1. *d* is almost independent of the ratio of SEBS-gMA/SEBS, implying that the addition of SEBS-gMA/SEBS has little effect on the lamellar thickness of PA6. *L* is also independent of the composition, except that in blend with 0/20 SEBS-gMA/SEBS; the blend with 0/20 SEBS-gMA/SEBS shows a larger *L*, whereas the other blends show a smaller *L*. The larger *L* in blend with 0/20 SEBS-gMA/SEBS may be ascribed to the increased amorphous thickness by incorporation of the PC component between PA crystalline lamellae. Combining the large *L* with a constant *d*, it may suggest that, in blend with 0/20 SEBS-gMA/SEBS, the PC component existing on the PA6-rich phases is trapped between PA crystalline lamellae. In a miscible semicrystalline polymer/amorphous polymer blend, the amorphous polymer is trapped between crystalline lamellae under a high

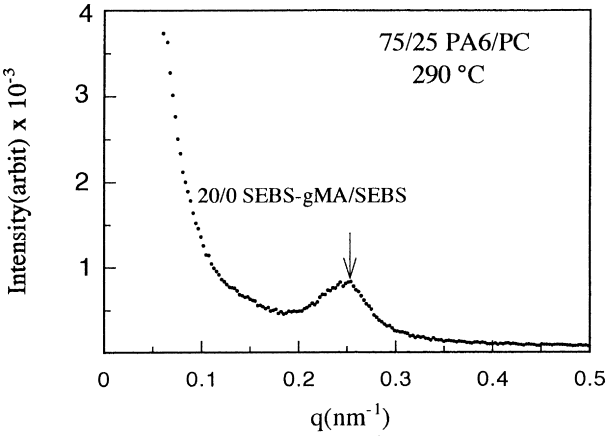

Fig. 3. SAXS intensity profile at 290°C in 75/25 PA6/PC blend with 0/20 SEBS-gMA/SEBS.

crystallization rate and thus L increases [11–15]. The PA6-rich phases containing PC seems to originate from the SD process, as discussed in Fig. 1. In general, the phase separation by SD consists of A-rich phases (B-poor phases) and B-rich phases (A-poor phases); a certain amount of B component is mixed in the A-rich phases.

From the values of d and L, the linear crystallinity w is obtained

$$w = d/L. \quad (1)$$

As shown in Table 1, the larger w in blend with 0/20 SEBS-gMA/SEBS suggests that the non-crystalline polymer PC is incorporated between the PA6 crystalline lamellae.

3.1.2. Small angle X-ray scattering

Fig. 3 shows the typical SAXS profile at 290°C, at which the PA crystallites were completely melted. All blends of added SEBS-gMA/SEBS showed a sharp peak at $q = 0.26\ \mathrm{nm}^{-1}$. The periodic length (24.2 nm) is obtained by applying Bragg's law to the peak position of the SAXS profile. The value was identical with the periodic length (25 nm) of the microphase separation calculated by TEM (see Table 1). The peak can then be ascribed to the periodic length of the microphase separation of SEBS-gMA/SEBS.

Fig. 4 shows the SAXS profiles in the injected sample. In pure 75/25 PA/PC blend without the addition of SEBS-gMA/SEBS, the scattering intensity decreases monotonously with q, suggesting that the PA6 crystalline lamellae are randomly oriented (a). The blend with 0/20 SBES-gMA/SEBS shows the sharp scattering peak at $q = 0.26\ \mathrm{nm}^{-1}$, whereas the other blends show the broad scattering peaks at the same q. One may mention two possibilities about the origin of the peak: one is the long period between two adjacent crystalline lamellae and the other is the periodic length of the microphase separation of SEBS-gMA/SEBS. The latter possibility seems to be more realistic, as the periodic length is identical with the distance between microdomains (24 nm) calculated by TEM. A supplemental evidence is clearly given by the results in Fig. 3. The periodic length, obtained by SAXS peak at 290°C above the PA melting point, was 24.2 nm the same as that of the injected sample.

As a measure of the sharpness of the SAXS profiles, as illustrated schematically in Fig. 5, one employs the ratio of the intensity at q_1 to that at q_2; i.e., $H = I(q_2)/I(q_1)$. The results of these calculations are depicted in Fig. 6. H in blend with 0/20 SEBS-gMA/SEBS shows a high value i.e., a sharp peak, whereas in other blends it shows a low value, i.e., broad peak. This is because of different location of SEBS-gMA/SEBS.

In blend with 0/20 SEBS-gMA/SEBS with partially miscible system, SEBS-gMA/SEBS locates in the PC-rich phases (see Fig. 2) so that the PA crystallization hardly influences the microphase-separated domain during cooling (crystallization) after injection mold. The periodic regularity of the microphase separation at high temperatures may then be kept.

In the other blends with immiscible system, SEBS-gMA/SEBS domains are located in the PA matrix. The PA crystallization during cooling may influence the structure of the microphase-separated domain; the crystalline lamellae grows up to penetrate into the microdomains and disorder

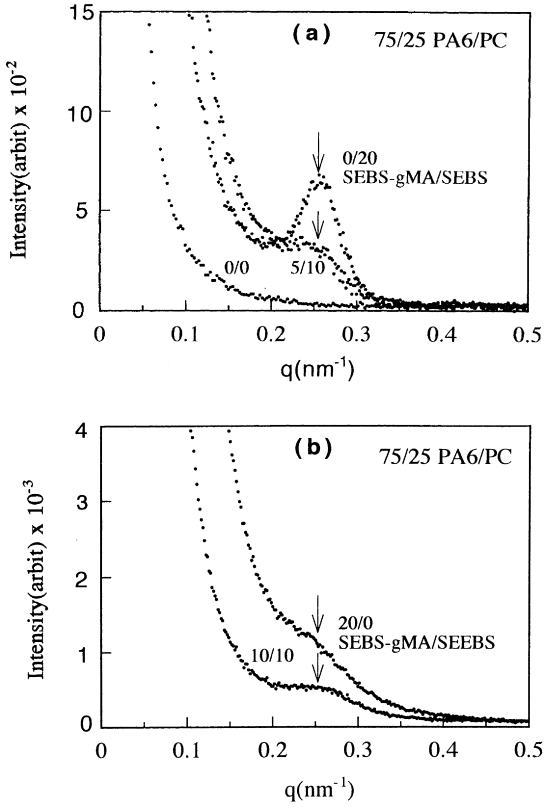

Fig. 4. SAXS intensity profiles in 75/25 PA6/PC blends with 0/0, 0/20, 5/15, 10/10 and 20/0 SEBS-gMA/SEBS.

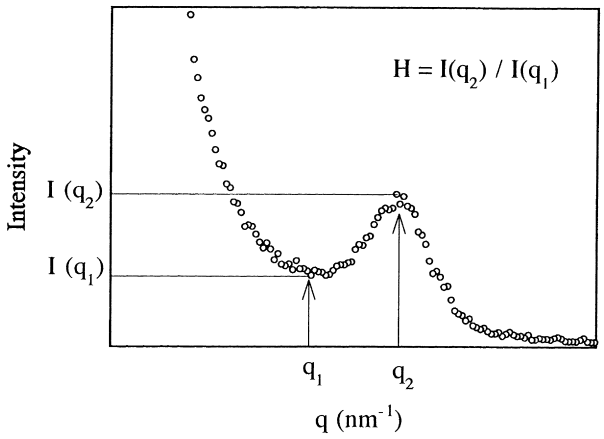

Fig. 5. Schematic diagram of definition of sharpness in a typical SAXS intensity profile.

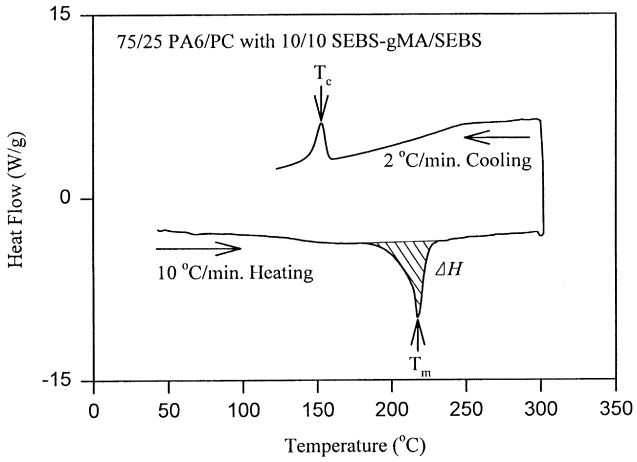

Fig. 7. DSC scan in 75/25 PA6/PC blend with 10/10 SEBS-gMA/SEBS.

the periodic regularity of the microphase separation, and then it causes the broad SAXS profile. The penetration of the PA6 lamellae into microdomain and the disordered periodic regularity are seen in Fig. 2(b)–(d).

3.2. Melting behavior and crystallinity

The melting behavior of the blends taken from the injection molded specimen was examined by DSC. All samples were heated to above melting, held at 300°C for 2 min to render the samples completely amorphous, and cooled from the melt with a cooling rate of 2°C/min^{-1}. Crystallization (T_c) and melting temperatures (T_m) were defined as the peak maximum or minimum of the exothermic or endothermic transitions, respectively. The typical DSC result is shown in Fig. 7. The values of T_m and T_c, obtained by DSC, are given in Fig. 8. It can be seen that the T_m is not much affected by the ratio of SEBS-gMA/SEBS. The T_m depends on crystalline lamellar thickness and defect [16]. The lamellar thickness d is constant and independent of the ratio of SEBS-gMA to SEBS (see Table 1). Therefore, the constant T_m may be interpreted by constant d.

The T_c decreases with the addition of SEBS-gMA/SEBS. Especially, the T_c in blend with 0/20 SEBS-gMA/SEBS shows the lower value. This may come from the SD structure in this blend composition, as discussed in Table 1. By SD, the PC component is contained in the PA-rich phases. In the PA-rich phases, the T_g increases by the existence of PC. Note that T_g in PC is higher than that in PA6. Higher T_g decreases the diffusion coefficient so that the crystallization rate is reduced. Crystallization rate consists of nucleation rate and diffusion rate. The existence of PC in the PA-rich phases by SD process may retard the crystallization rate and thereby the T_c in blend with 0/20 SEBS-gMA/SEBS can be decreased.

In general, the degree of overall crystallinity of crystallizable polymer materials can be estimated by measuring the enthalpic change at melt. The result is shown in Fig. 9. As expected, the melting enthalpy by the addition of the SEBS-gMA/SEBS is decreased. This is certainly attributable to the decrease in the amount of crystalline polymer PA6. In blend with 0/20 SEBS-gMA/SEBS, the heat of fusion drastically decreased; heat of fusion, i.e., crystallinity, in this blend is lower than those in other blends. It can be deduced that the

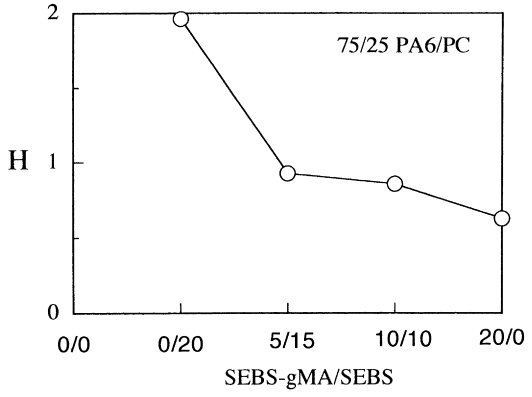

Fig. 6. H plotted against the ratios of SEBS-gMA to SEBS in 75/25 PA6/PC blend.

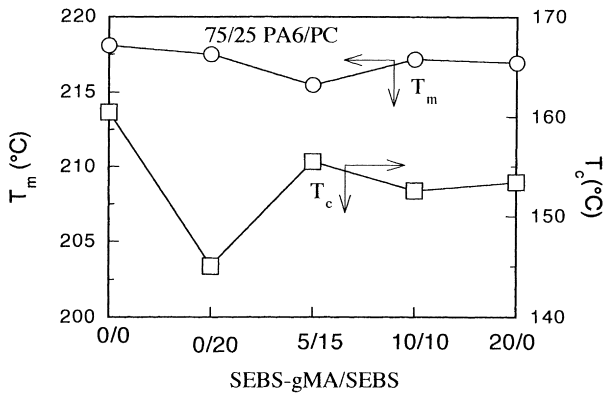

Fig. 8. T_m and T_c plotted against the ratio of SEBS-gMA to SEBS in 75/25 PA6/PC blend.

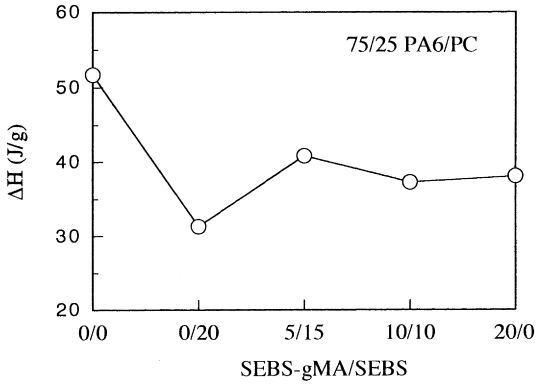

Fig. 9. Δ*H* plotted against the ratio of SEBS-gMA to SEBS in 75/25 PA6/PC blend.

PA crystallinity is decreased by incorporation of the non-crystalline PC component in the PA6-rich phases. In blend with 0/20 SEBS-gMA/SEBS, the non-crystalline polymer PC may be contained in the PA-rich phases by SD as discussed in Table 1. The linear crystallinity *w* in Table 1 exhibits identical SEBS-gMA/SEBS dependence and thereby further support above interpretation.

4. Conclusions

Phase morphology in the melt-injected blend of 75/25 PA6/PC blends with 0/20, 5/15, 10/10 and 20/0 SEBS-gMA/SEBS was investigated by SAXS and TEM. Then, it was found that the 75/25 PA6/PC blend with 0/20 SEBS-gMA/SEBS shows the co-continuous structure, i.e., SD structure, which takes place in the partially miscible system. The other blends showed that the PC macrodomains and SEBS/SEBS-gMA microdomains were dispersed in the PA6 matrix, indicating that these blends are totally immiscible. By a series of crystalline morphology by SAXS, TEM and DSC analyzes, it was revealed that 75/25 PA6/PC blend with 0/20 SEBS-gMA/SEBS showed the low crystallinity and crystallization temperature, and the high periodic regularity of SEBS-gMA/SEBS microphase separation. However, the 75/25 PA6/PC blends with 5/15, 10/10 and 20/0 SEBS-gMA/SEBS showed the high crystallinity and crystallization temperature, and the low periodic regularity of SEBS-gMA/SEBS microphase separation. This different behavior could be interpreted by the co-continuous phase morphology with partially miscible system in blend with 0/20 SEBS-gMA/SEBS and the matrix/domain phase morphology with completely immiscible system in the other blends.

References

[1] Gattiglia E, Turturro A, Pedemonte E. J Appl Polym Sci 1989;38:1807.
[2] Gattiglia E, Turturro A, Pedemonte E, Dondero G. J Appl Polym Sci 1990;41:1411.
[3] Horiuchi S, Matchariyakul N, Yase K, Kitano T, Choi HK, Lee YM. Polymer 1996;37:3065.
[4] Horiuchi S, Matchariyakul N, Yase K, Kitano T, Choi HK, Lee YM. Polymer 1997;38:59.
[5] Horiuchi S, Matchariyakul N, Yase K, Kitano T, Choi HK, Lee YM. Polymer 1997;38:6317.
[6] Coppola F, Greco R, Martuscelli E. Polymer 1988;29:963.
[7] Koberstein JJ, Morra B, Stein RS. J Appl Crystallogr 1980;13:34.
[8] Okamoto M, Inoue T. Polymer 1994;35:257.
[9] Okamoto M, Shiomi K, Inoue T. Polymer 1995;36:1.
[10] Okamoto M, Inoue T. Polymer 1995;14:2739.
[11] Keith HD, Padden Jr. FJ. J Appl Phys 1964;35:1270.
[12] Keith HD, Padden Jr. FJ. J Appl Phys 1963;34:2409.
[13] Warner FP, Macknight WJ, Stein RS. J Polym Sci, Polym Phys Edn 1977;15:2113.
[14] Stein RS, Khambatta FB, Warner FP, Russell TP, Escala A, Balizer E. J Polym Sci, Polym Phys Edn 1978;63:313.
[15] Hudson SD, Davis DD, Lovinger AJ. Macromolecules 1992;25:1759.
[16] Wunderlich B. Macromolecular Physics, ch. 3.2. New York: Academic Press, 1973.